NJC

Accepted Manuscript

This is an *Accepted Manuscript*, which has been through the Royal Society of Chemistry peer review process and has been accepted for publication.

Accepted Manuscripts are published online shortly after acceptance, before technical editing, formatting and proof reading. Using this free service, authors can make their results available to the community, in citable form, before we publish the edited article. We will replace this *Accepted Manuscript* with the edited and formatted *Advance Article* as soon as it is available.

You can find more information about *Accepted Manuscripts* in the Information for Authors.

Please note that technical editing may introduce minor changes to the text and/or graphics, which may alter content. The journal's standard Terms & Conditions and the Ethical guidelines still apply. In no event shall the Royal Society of Chemistry be held responsible for any errors or omissions in this *Accepted Manuscript* or any consequences arising from the use of any information it contains.

ROYAL SOCIETY OF CHEMISTRY

www.rsc.org/njc

Journal Name

ARTICLE

New conjugated molecules with four DPP (diketopyrrolopyrrole) moieties linked by [2,2]paracyclophane as electron acceptors for organic photovoltaic cells

Received 00th January 20xx,
Accepted 00th January 20xx

DOI: 10.1039/x0xx00000x

www.rsc.org/

Yang Yang, Guanxin Zhang,* Chenmin Yu, Jingjing Yao, Zitong Liu, Deqing Zhang*

In this paper we report two conjugated molecules **1** and **2** with four diketopyrrolopyrrole (DPP) moieties which are linked by [2,2]paracyclophane. Highest Occupied Molecular Orbital (HOMO) and Lowest Unoccupied Molecular Orbital (LUMO) energies of **1** and **2** were estimated with the respective onset oxidation and reduction potentials which were determined on the basis of the cyclic voltammetric data. **1** and **2** show strong absorptions in the visible region. Blending thin films of **1** and **2** with P3HT (poly(3-hexylthiophene)) at different weight ratios were utilized as active layers to fabricate solar cells. The results reveal that blending thin films of P3HT/**1** and P3HT/**2** at a weight ratio of 2:1 yielded the best photovoltaic performance with power conversion efficiencies (PCEs) up to 1.33% and 1.84% after thermal annealing. The blending thin films of P3HT/**1** andP3HT/**2** were characterized with XRD (X-ray diffraction) and AFM (Atomic Force Microscope) techniques. The low inter-chain packing order degree and poor thin film morphology are responsible for the relatively low PCEs.

Introduction

The performances of organic photovoltaic cells (OPVs) are dependent on the features of electron donors and acceptors. Various small and polymeric electron donors and acceptors have been explored for high-performance photovoltaic materials.[1-5] Fullerene-derivatives including $PC_{61}BM$ and $PC_{71}BM$ are widely utilized as electron acceptors for OPVs since they show high electron affinity, high electron mobility and isotropic charge-transporting.[6] However, HOMO/LUMO energies of fullerene molecules are not easily tuned by chemical modifications to match the electron donors to maximize the open-circuit voltage (V_{OC}) and minimize the energy loss. Importantly, fullerenes usually show weak absorptions in the visible region.[7] Accordingly, non-fullerene acceptors with strong absorptions in the visible region and appropriate HOMO/LUMO levels have been explored in recent years.[8-13] These efforts yielded promising non-fullerene acceptors which are expected to pair with electron donors according to their energy levels and absorptions to form OPVs of high power conversion efficiencies (PCEs). Nevertheless, only a limited number of non-fullerene small molecule acceptors were successfully used to fabricate OPVs with PCEs higher than 1.5% and even fewer with PCEs higher than 2.5%.[9-12] A few perylene diimide derivatives led to OPVs with PCEs higher than 5.0%.[13]

It is known that DPP (diketopyrrolopyrrole) shows strong absorptions in the visible region and HOMO/LUMO energies can be tuned by connection with electron donating or accepting moieties. In fact, a number of DPP-entailing small conjugated molecules and polymers were investigated as electron donors for OPVs.[14-17] Some of us have very recently described new conjugated molecular scaffold based on [2,2]paracyclophane with four DPP moieties and the new conjugated molecules can function as electron acceptors for organic photovoltaic cells.[18] In this paper, we describe two conjugated molecules **1** and **2** (Scheme 1) in which four DPP moieties are linked at different positions of [2,2]paracyclophane. The selection of [2,2]paracyclophane framework is owing to its cylindrical and rigid structure which is expected to be beneficial for intermolecular packing and thus charge transporting. The presence of four DPP moieties is anticipated to be favourable for the formation of more donor-acceptor interfaces. The connection of electron withdrawing 3,4,5-triflurophenyl moieties in **2** is intended to tune the HOMO/LUMO levels. The results reveal that both **1** and **2** can function as electron acceptors for organic photovoltaic cells.

Results and discussions

Synthesis and characterization

The synthesis of **1** and **2** is outlined in Scheme 1. Compounds **4**[19] and **5**[18] were synthesized according to the reported procedure. Then, Sonogashira coupling of 4,5,13,14-

Beijing National Laboratory for Molecular Sciences, Organic Solids Laboratory, Institute of Chemistry, Chinese Academy of Sciences, Beijing 100190, China.
E-mail: dqzhang@iccas.ac.cn
Electronic Supplementary Information (ESI) available: TGA, IPCE, NMR and other additional data,See DOI: 10.1039/x0xx00000x

Journal Name

ARTICLE

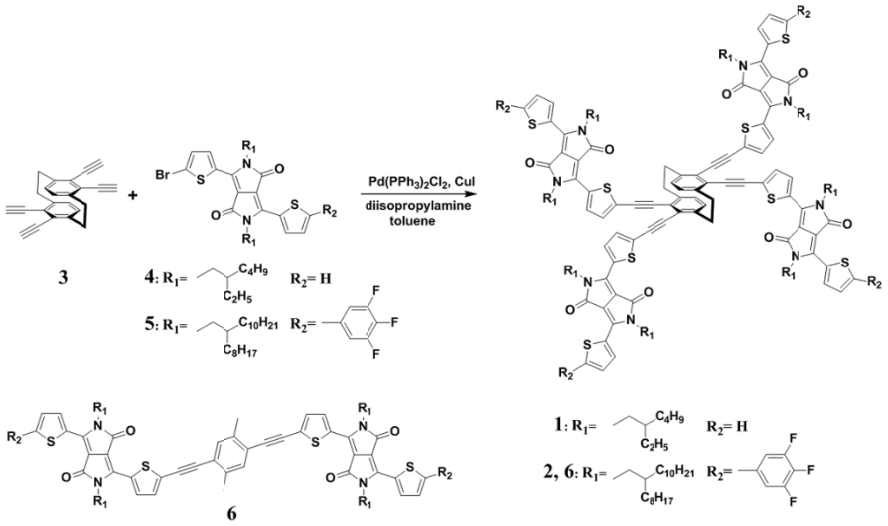

Scheme 1 Chemical structures of **1** and **2** as well as their synthetic approach.

Tetraethynyl [2,2]paracyclophane (**3**) with **4** and **5** separately yielded **1** and **2** in acceptable yields (see Experimental section). The chemical structures and purities of **1** and **2** were established and confirmed by spectroscopic data and elemental analysis (see Experiment section). **1** and **2** show good solubilities in common organic solvents such as chloroform, tetrahydrofuran, toluene and *o*-DCB (1,2-dichlorobenzene) at room temperature. Thermogravimetric analysis (TGA) reveals that **1** and **2** are thermally stable below 300 °C (see Figure S1).

HOMO/LUMO energies and bandgaps

As depicted in Figure 1a, both **1** and **2** exhibit two reversible oxidation waves and one reduction wave. Based on the respective onset oxidation and reduction potentials, the highest occupied molecular orbital (HOMO) and the lowest unoccupied molecular orbital (LUMO) energies of **1** and **2** were estimated by the following equations and listed in Table 1: HOMO = $-(E_{onset}^{ox1} + 4.8)$ eV and LUMO = $-(E_{onset}^{red1} + 4.8)$ eV. HOMO/LUMO energies of **1** and **2** were estimated to be -3.41 eV/-5.27 eV and -3.43 eV/-5.30 eV, respectively (see Table 1). Accordingly, bandgaps of **1** and **2** were calculated to be 1.86 eV and 1.87 eV, respectively. Obviously, both HOMO and LUMO levels of **2** are lower than those of **1**. This is owing to the electron withdrawing effect of 3,4,5-triflurophenyl groups in **2**. HOMO/LUMO energies of **1** and **2** were compared with those of P3HT as depicted in Fig. 1b. Judging from the energy levels, both **1** and **2** are suitable electron acceptors for OPVs in combination with P3HT (poly(3-hexylthiophene)) as the electron donor. In particular, the energy differences between the HOMO level of P3HT and those of **1** or **2** are higher than 1.2 eV, which may result in relatively high open-circuit voltage (V_{OC}).

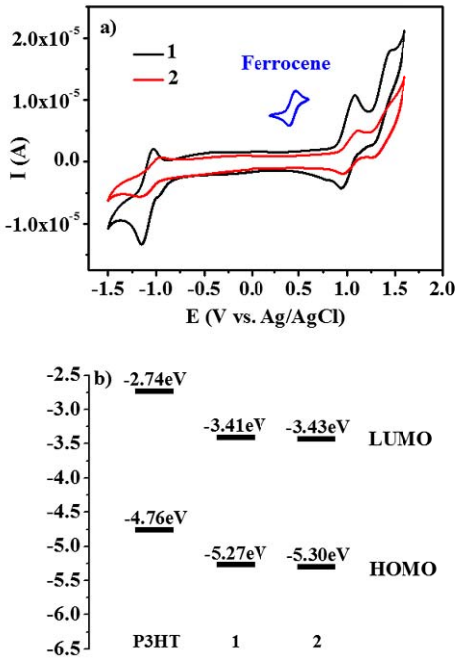

Fig. 1 a) Cyclic voltammograms of **1** and **2** in CH_2Cl_2 (1.0×10^{-3} M) at a scan rate of 100 mV/s with n-Bu_4NPF_6 (0.1 M) as the supporting electrolyte; b) HOMO/LUMO energies for **1**, **2** and P3HT.

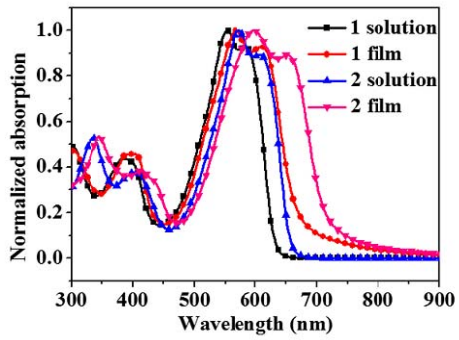

Fig. 2 The normalized absorption spectra for solutions of **1** (1.0×10^{-5} M in CH_2Cl_2) and **2** (1.0×10^{-5} M in CH_2Cl_2) and their thin films.

As expected, both **1** and **2** show strong absorptions in the visible region as shown in Fig. 2. For instance, the solution of **1** exhibits absorptions in the range of 450-650 nm and the strong absorption around 550 nm with ε_{max} = 213000 M^{-1} cm^{-1}. The absorption maxima of **1** and **2** are listed in Table 1. Compared to those in solutions, the absorption spectra of the thin-films of **1** and **2** are red-shifted. The absorption band at 550 nm and 585 nm in solution are shifted to 567 nm and 611 nm for the thin-film of **1**. Thin film of **2** absorbs strongly around 600 nm and 650 nm which are red-shifted in comparison with those in solution. Such absorption spectral shifts are probably induced by the intermolecular pi-pi interactions within thin films. The absorption spectra of **2** in both solution and thin film are red-shifted in comparison with those of **1**. This can be interpreted by considering the presence of 3,4,5-triflurophenyl groups in **2** which may elongate the conjugation length. Additionally, the optical bandgaps of **1** and **2** were estimated to be 1.85 eV and 1.74 eV on the basis of the respective onset absorptions of thin-films of **1** and **2**. These are in good agreement with those obtained based on their cyclic voltammetric data (see Table 1).

Table 1. Absorption maxima, redox potentials, HOMO/LUMO energies and bandgaps of **1** and **2**.

Compd.	λ_{max} [nm] solution [a]	film	E_{onset}^{ox1} [V] [c]	E_{onset}^{red1} [V] [c]	HOMO [eV] [d]	LUMO [eV] [d]	band gap [eV]
1	551(213000), 585(198000) [b]	567, 611	0.47	-1.39	-5.27	-3.41	1.85 [e] (1.86) [f]
2	572(219000), 608(196000) [b]	599, 651	0.50	-1.37	-5.30	-3.43	1.74 [e] (1.87) [f]

a) Measured in CH_2Cl_2 solutions for **1** and **2** with a concentration of 1.0×10^{-5} M; b) Molar extinction coefficient (ε_{max}, M^{-1} cm^{-1}); c) Onset potentials (V *vs.* Fc/Fc^+) for oxidation (E_{onset}^{oxl}) and reduction (E_{onset}^{redl}). d) Calculated based on the respective onset oxidation and reduction potentials of **1** and **2** with the following equations: HOMO = $-(E_{onset}^{ox1} + 4.8)$ eV and LUMO = $-(E_{onset}^{red1} + 4.8)$ eV; e) based on the onset absorption data of thin films; f) based on the redox potentials.

Photovoltaic device performance

To demonstrate potential applications of **1** and **2** as electron acceptors for OPVs, the blending thin films of **1** and **2** with P3HT were utilized to fabricate OPVs with the conventional configuration of indium tin oxide (ITO)/poly(3,4-ethylenedioxythiophene):poly(styrene sulfonate) (PEDOT:PSS) /active layer/Ca/Al. The respective photovoltaic performance data based on the *J-V* curves shown in Fig. 3 are summarized in Table 2. The pairing of **1** with P3HT yielded OPVs with V_{OC} of 1.03-1.06 V, thanks to the large energy level difference between the HOMO of P3HT and LUMO of **1**. Both **1** and **2** were blended with P3HT separately for different weight ratios and tested as active layers for OPVs. Table 2 lists the respective photovoltaic performance data. The blending P3HT/**1** at a weight ratio of 2:1 gave the best performance: V_{OC} = 1.03 V, J_{SC} = 2.36 mA cm^{-2}, FF = 0.41 and PCE = 0.99%. Thermal annealing of the blending thin films at 110 °C for 10 min. increased J_{SC} to 2.93 mA cm^{-2} and FF was also slightly enhanced (see Table 2), thus leading to PCE of 1.33%. Similarly, the blending thin film of P3HT and **2** at weight ratio of 2:1 gave the best performance as well: V_{OC}, J_{SC}, FF and PCE reached 0.93 V, 3.27 mA cm^{-2}, 0.47 and 1.45%, respectively. The PCE increased to 1.84% after thermal annealing of the photoactive thin film at 110 °C for 10 min. Introduction of additives could not obviously improve the photovoltaic performances for the blending thin films of **1** and **2** with P3HT under current device configuration. For comparison, OPVs with thin films of P3HT/PC_{61}BM was also fabricated under the same conditions. After optimization, the P3HT/PC_{61}BM blending thin film at weight ratio of 1:1 yielded PCE of 3.98%. Thus, the OPV with **2** as a non-fullerene acceptor can reach 46% of PCE of that with P3HT/PC_{61}BM as the active layer. According to our previous report,[18] the PCE of OPVs with the blending film of P3HT with **6** (Scheme 1) at a weight ratio of 1:1 was just 0.90%. Compound **6** contains no [2,2]paracyclophane framework. Thus, it may be concluded that the incorporation of [2,2]paracyclophane framework in **1** and **2** is beneficial for better photovoltaic performance after blending with P3HT.

Fig. S2 shows the IPCE (incident photon to converted current efficiency) spectra of the blending thin films of P3HT/**1** and P3HT/**2** at different weight ratios before and after thermal annealing. The profiles of IPCE spectra correspond well to the respective absorption spectra of thin films of **1** and **2**, implying that **1** and **2** within the blending thin films make considerable contribution to IPCE. The blending thin films of **1** and **2** with P3HT at a weight ratio of 2:1 yielded higher IPCE. Moreover, IPCE was enhanced after thermal annealing of the blending thin films. The maxima IPCEs of 14% (at 562 nm) and 27% (at 558 nm) were observed for the blending thin films P3HT/**1** and P3HT/ **2**, respectively. This may partly explain the observation that thin film of P3HT/**2** shows higher PCE than that of P3HT/**1**.

Journal Name

ARTICLE

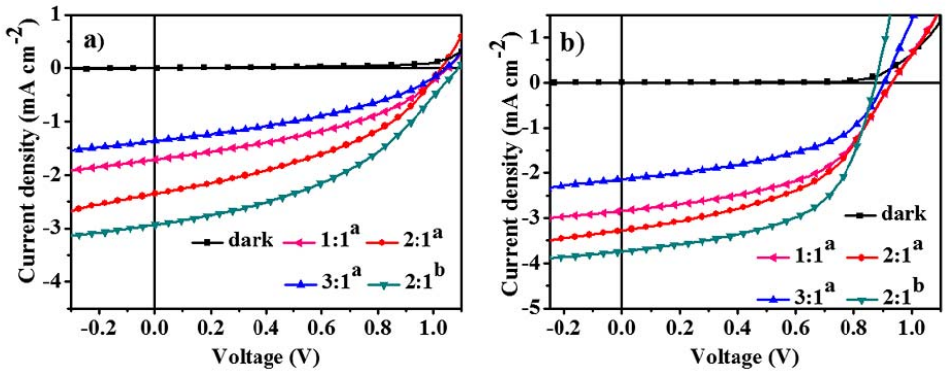

Fig. 3 *J-V* curves of OPVs based on P3HT/**1** (a) and P3HT/**2** (b) with different weight ratios under the illumination of AM 1.5G, 100 mW cm^{-2}.

Table 2. The device data of OPVs based on P3HT/**1** and P3HT/**2** under the illumination of AM 1.5G, 100 mW cm^{-2}.

Donor/acceptor	w/w	V_{OC} [V]	J_{SC} [mA cm^{-2}]	FF	Best PCE [%]	Average PCE [c] [%]
P3HT/**1**	1:1 [a]	1.04	1.71	0.40	0.72	0.66
	2:1 [a]	1.03	2.36	0.41	0.99	0.97
	3:1 [a]	1.04	1.36	0.38	0.54	0.50
	2:1 [b]	1.06	2.93	0.42	1.33	1.20
P3HT/**2**	1:1 [a]	0.93	2.83	0.51	1.34	1.24
	2:1 [a]	0.93	3.27	0.47	1.45	1.42
	3:1 [a]	0.90	2.14	0.48	0.95	0.90
	2:1 [b]	0.87	3.73	0.56	1.84	1.76

[a] Without thermal annealing; [b] after thermal annealing at 110 °C for 10 min.; [c] The average values of the PCE based on more than 10 devices.

The charge mobilities of the blending thin films of P3HT/**1** and P3HT/**2** were measured with space-charge-limited-current (SCLC) method.[20] For hole-only and electron-only devices, the structures of ITO/PEDOT:PSS/P3HT:**1** (or **2**) (2:1, w/w)/Au and Mg/P3HT:**1** (or **2**) (2:1, w/w)/Mg were used, respectively. The large energy barriers (1.69 eV and 1.67 eV for **1** and **2**) between Au work function (5.1 eV) and LUMO levels (-3.41 eV and -3.43 eV for **1** and **2**) of **1** and **2** would suppress the electron injection from the top electrode, and thus render the devices hole-only characteristic. Similarly, the large energy barriers (1.61 eV and 1.64 eV for **1** and **2**) between Mg work function (3.66 eV) and HOMO levels (-5.27 eV and -5.30 eV for **1** and **2**) of **1** and **2** would suppress the hole injection; in comparison, the respective electron injection barriers are quite small (0.25 eV and 0.23 eV for **1** and **2**), and thus render the devices electron-only characteristic.

Table S1 lists the hole and electron mobilities of the blending thin films of P3HT/**1** and P3HT/**2** at a weight ratio of 2:1 before and after thermal annealing at 110 °C for 10 min. Hole mobilities are much higher than the respective electron mobilities for both P3HT/**1** and P3HT/**2** thin films, thus hole and electron transporting are not balanced within these thin films. This may be responsible for low PCEs for these blending thin films. Both hole and electron mobilities increase after thermal annealing. For instance, for P3HT/**2** thin film, μ_h increases from 1.87×10^{-4} $cm^2V^{-1}s^{-1}$ to 3.48×10^{-4} $cm^2V^{-1}s^{-1}$, and μ_e increases from 4.48×10^{-7} $cm^2V^{-1}s^{-1}$ to 1.30×10^{-6} $cm^2V^{-1}s^{-1}$. This agrees well with the observation that photovoltaic performances of P3HT/**1** and P3HT/**2** are improved after thermal annealing (see Table 2). Compared to P3HT/**1** thin film, the blending thin film of P3HT/**2** exhibits higher hole and electron mobilities, in particular after thermal annealing; moreover, the ratio of μ_h/μ_e of P3HT/**2** is lower than that of P3HT/**1** both before and after thermal annealing as listed in Table S1. These results explain the fact that P3HT/**2** thin film yields higher PCE than P3HT/**1** thin film (see Table 2).

The blending thin films of P3HT/**1** and P3HT/**2** at a weight ratio of 2:1 were also investigated with XRD and AFM

techniques. As depicted in Fig. S3, a signal at 2θ = 5.40°, corresponding the *d*-spacing of 16.3 Å, was detected for both blending thin films, and the intensity was slightly enhanced after thermal annealing. Furthermore, a weak diffraction at 2θ = 21.3°, corresponding the *d*-spacing of 4.0 Å, was detected for both P3HT/**1** and P3HT/**2**. These XRD signals are probably owing to the formation of crystalline domains of P3HT within the blending thin films according to previous studies,[21] in which a diffraction signal at 2θ = 5.40° was reported forP3HT/$PC_{61}BM$ thin film on PEDOT:PSS. It is noted that these diffractions are rather weak and thus the inter-chain packing order degree is low for both P3HT/**1** and P3HT/**2**.

The surface morphologies of P3HT/**1** and P3HT/**2** blending thin films were also examined with AFM in tapping mode. Based on the AFM images shown in Fig. 4, the root-mean-square (rms) roughness for the P3HT/**1** thin film decreases from 3.58 nm to 2.56 nm after thermal annealing. Similarly, the rms roughness for the P3HT/**2** thin film decreases from 3.22 nm to 2.35 nm after thermal annealing. The bright and dark domains in the AFM phase images become more clearly separated after thermal annealing for both of P3HT/**1** and P3HT/**2** thin films. Moreover, sizes of bright domains are varied from 50-80 nm to 25-50 nm for P3HT/**1** thin film, whereas those of P3HT/**2** thin film are reduced to about 50 nm after thermal annealing. These AFM images are consistent with the observation that thermal annealing led to the improvement of PCEs for both thin films according to the previous studies.[8d] However, the phase separation for both thin films is not clear and uniform even after thermal annealing. This may be the main reason why blending thin films of P3HT/**1** and P3HT/**2** display low photovoltaic performance.

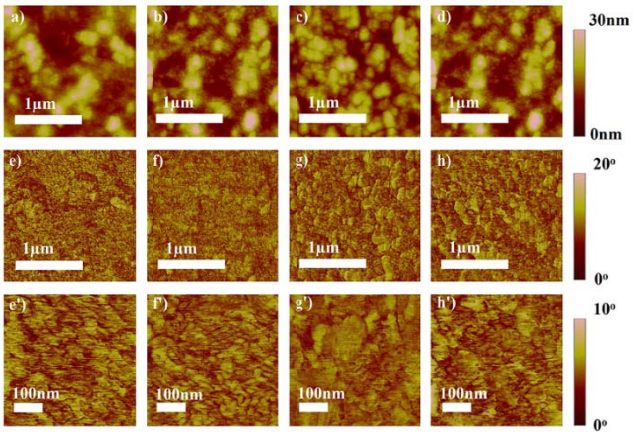

Fig. 4 AFM height (a-d) and phase (e-h) images (2 μm × 2 μm) of P3HT/**1** (2:1, w/w) blending films without (a, e) and with thermal annealing (b, f) and P3HT/**2** (2:1, w/w) blending films without (c, g) and with thermal annealing (d, h); AFM phase images (500 nm×500 nm) of P3HT/**1** (2:1, w/w) blending films without (e') and with thermal annealing (f') and P3HT/**2** (2:1, w/w) blending films without (g') and with thermal annealing (h').

Conclusions

Four diketopyrrolopyrrole (DPP) moieties were successfully incorporated into the [2,2]paracyclophane led to new conjugated molecules **1** and **2**. On the basis of cyclic voltammetric data, lowest unoccupied molecular orbital (LUMO) and highest occupied molecular orbital (HOMO) energies of **2** were lower than those of **1** because of the electron withdrawing moieties of 3,4,5-triflurophenyl in **2**. Both **1** and **2** can function as electron acceptors for photovoltaic cells. Blending thin films of **1** and **2** with P3HT (poly(3-hexylthiophene)) were tested at different weight ratios as active layers to fabricate OPVs with the conventional device configuration. The results reveal that blending thin films of P3HT/**1** and P3HT/**2** at a weight ratio of 2:1 yielded the best photovoltaic performance with power conversion efficiencies (PCEs) up to 1.33% and 1.84% after thermal annealing. XRD (X-ray diffraction) and AFM (Atomic Force Microscope) characterization of the blending thin films manifests that the inter-chain packing order degree is low and the thin film morphology for these blending thin films is poor even after thermal annealing. These structural features of these blending thin films may explain low charge mobilities and PCEs of P3HT/**1** and P3HT/**2** thin films. Optimization of thin film morphology is underway to improve PCEs. Connection of strong electron accepting moieties and alteration of alkyl chains may offer new electron acceptors to pair with polymeric donors for organic photovoltaic cells (OPVs) of high performance.

Experimental section

Materials and characterization techniques

Chemicals were purchased from Alfa-Aesar and Sigma-Aldrich, and used without further purification. Solvents and other common reagents were obtained from Beijing Chemical Co.. 4,5,13,14-Tetraethynyl[2,2]paracyclophane (**3**) was synthesized according to the reported procedures.[22]

^{1}H NMR and ^{13}C NMR spectra were measured on a Bruker AVANCE III 400 MHz spectrometer. Elemental analysis of carbon, hydrogen, sulfur and nitrogen was performed on a Carlo Erba model 1160 elemental analyzer. UV-vis absorption spectra were measured with JASCO V-570 UV-Vis spectrophotometer. TGA-DTA measurements were carried out on a SHIMADZU DTG-60 instruments under a dry nitrogen flow, heating from room temperature to 550 °C, with a heating rate of 10 °C/min. Cyclic voltammetric measurements were carried out in a conventional three-electrode cell using a Pt working electrode, a Pt counter electrode and a Ag/AgCl (saturated KCl) reference electrode on a computer-controlled CHI660C instruments at room temperature; the scan rate was 100 $mV{\cdot}s^{-1}$, and *n*-Bu_4NPF_6 (0.1 M) was used as the supporting electrolyte. For calibration, the redox potential of ferrocene/ferrocenium (Fc/Fc^{+}) was measured under the same conditions. The onset oxidation and reduction potentials were presented by reference to the redox potential of ferrocene/ferrocenium (Fc/Fc^{+}).

X-ray diffraction (XRD) measurements were carried out in the reflection mode at room temperature, using a 2-kW Rigaku X-ray diffraction system. Atomic force microscopy (AFM) images of the thin films were obtained on a NanoscopeIIIa AFM (Digital instruments) operating in tapping mode. AFM samples and microscopic images were identical to those used in organic solar cells.

Synthesis

Synthesis of 1. To the solution of **3** (30 mg, 0.1 mmol) and **4** (300 mg, 0.5 mmol) in 25 mL of anhydrous toluene deoxygenated with nitrogen, $Pd(PPh_3)_2Cl_2$ (14 mg, 0.02 mmol) , CuI (3.8 mg, 0.02 mmol) and diisopropylamine (6.0 mL) were added under nitrogen. The mixture was heated at 75 ^oC for 12 h under nitrogen atmosphere. After cooling to room temperature, the solvent was evaporated under vacuum and the residue was subjected to silica gel column chromatography with petroleum ether (60-90 ^oC)/CH_2Cl_2 (v/v, 1/1) as eluent. Compound **1** was obtained as a purple-red solid (35 mg) in 15% yield.

^1H NMR (400 MHz, $CDCl_3$) δ 8.95 (d, *J* = 3.4 Hz, 4H), 8.88 (d, *J* = 3.4 Hz, 4H), 7.66 (d, *J* = 5.0 Hz, 4H), 7.49 (d, *J* = 4.0 Hz, 4H), 7.30 - 7.28 (m, 4H), 7.02 (s, 4H), 4.07 – 4.03 (m, 16H), 3.60 – 3.57 (m, 4H), 3.19 – 3.16 (m, 4H), 1.89 (br, 8H), 1.37 – 1.25 (m, 64H), 0.92 – 0.82 (m, 48H). ^{13}C NMR (101 MHz, $CDCl_3$) δ 161.83, 161.74, 142.70, 141.16, 139.01, 135.86, 135.33, 133.06, 131.36, 131.05, 129.95, 128.67, 128.10, 127.11, 109.23, 108.26, 96.42, 90.82, 46.11, 39.42, 39.24, 33.17, 30.44, 30.40, 28.60, 28.52, 23.79, 23.70, 23.21, 14.20, 14.17, 10.68, 10.64. MALDI-TOF: 2394.6 ($M+H^+$); Anal. calcd. for $C_{144}H_{168}N_8O_8S_8$: C, 72.20; H, 7.07; N, 4.68; S, 10.71; found: C, 71.83; H, 7.04; N, 4.62; S, 10.45.

Synthesis of 2. Compound **2** was synthesized as for compound **1** and obtained as a violet solid in 15% yield.

^1H NMR (400 MHz, CD_2Cl_2) δ 8.90 (s, 8H), 7.54 (d, *J* = 4.0 Hz, 4H), 7.41 (d, *J* = 4.0 Hz, 4H), 7.33 – 7.23 (m, 8H), 7.04 (s, 4H), 3.99 (m, 16H), 3.61 (m, 4H), 3.18 (m, 4H), 1.91 (s, 8H), 1.30 – 1.14 (m, 256H), 0.86 – 0.78 (m, 48H). ^{13}C NMR (101 MHz, $CDCl_3$) δ 161.65, 153.09, 150.59, 150.53, 145.78, 142.63, 141.14, 139.87, 139.42, 138.78, 136.69, 135.58, 133.05, 131.31, 131.11, 130.26, 129.96, 129.51, 128.62, 128.47, 127.21, 125.72, 110.47, 110.24, 109.26, 109.07, 96.70, 90.87, 46.50, 38.17, 33.19, 32.07, 32.02, 31.53, 31.40, 30.26, 30.22, 29.88, 29.83, 29.79, 29.73,29.54, 29.51, 29.47, 26.61, 26.44, 22.83, 14.25. MALDI-TOF: 4262.2 (M^+); Anal. calcd. for $C_{264}H_{364}F_{12}N_8O_8S_8$: C, 74.39; H, 8.61; N, 2.63; S, 6.02; found: C, 74.37; H, 8.83; N, 2.67; S, 5.74.

Fabrication of organic photovoltaic cells

Solar cells were fabricated with a general structure of ITO/PEDOT:PSS (30 nm)/active layer/Ca (20 nm)/Al (70 nm). The patterned indium tin oxide (ITO) glass substrates were pre-cleaned by sequential ultrasonic treatments in detergent, deionized water, acetone, and isopropanol, and treated in ultraviolet-ozone chamber (Jelight Company, USA) for 20 min. A thin layer (30 nm) of poly(3,4-ethylenedioxythiophene):poly(styrene sulfonate) (PEDOT:PSS, Baytron P VP AI 4083, Germany) was spin-coated onto ITO glass substrates and baked at 150 ^oC for 15 min. Solutions of P3HT/**1** and P3HT/**2**, with different weight ratios was separately spin-coated on PEDOT:PSS layer to form the respective photoactive layers (ca. 80-100 nm). The thickness of the photoactive layer was measured by Ambios Technology XP-2 profilometer. Calcium (ca. 20 nm) and aluminum (ca. 70 nm) layers were then evaporated onto the surface of active layer under vacuum (ca. 10^{-5} Pa) to form the negative electrode. The active area of the device was 4.0 mm^2. *J–V* curves were measured with a computer-controlled Keithley 236 Source Measure Unit. A xenon lamp coupled with AM 1.5 solar spectrum filters was used as the light source, and the optical power at the sample was 100 mW cm^{-2}. The incident photon to converted current efficiency (IPCE) spectrum was measured by a Stanford Research Systems model SR830 DSP lock-in amplifier coupled with a WDG3 monochromator and 500 W xenon lamp.

Acknowledgements

The present research was financially supported by NSFC and the Strategic Priority Research Program of the Chinese Academy of Sciences, Grant No.XDB12010300. The authors thank Prof. Yongfang Li for helpful discussions and allowance for using the facility for fabrication of OPVs.

Notes and references

1 a) G. Yu, J. Gao, J. C. Hummelen, F. Wudl, A. J. Heeger, *Science*, 1995, **270**, 1789; b) J. Roncali, *Acc. Chem. Res.*, 2009, **42**, 1719; c) Y. Y. Liang, L. P. Yu, *Acc. Chem. Res.*, 2010, **35**, 1227; d) Y. F. Li, *Acc. Chem. Res.*, 2012, **45**, 723; e) A. Mishra, P. Bäuerle, *Angew. Chem. Int. Ed.*, 2012, **51**, 2020.

2 a) Y. Z. Lin, Y. F. Li, X. W. Zhan, *Chem. Soc. Rev.*, 2012, **41**, 4245; b) J. E. Coughlin, Z. B. Henson, G. C. Welch, G. C. Bazan, *Acc. Chem. Res.*, 2014, **47**, 257; c) L. Ye, S. Q. Zhang, L. J. Huo, M. J. Zhang, J. H. Hou, *Acc. Chem. Res.*, 2014, **47**, 1595; d) M. M. Li, W. Ni, X. J. Wan, Q. Zhang, B. Kan, Y. S. Chen, *J. Mater. Chem. A*, 2015, **3**, 4765; e) W. Ni, X. J. Wan, M. M. Li, Y. C. Wang, Y. S. Chen, *Chem. Commun.*, 2015, **51**, 4936.

3 a) J. B. You, L.T. Dou, K. Yoshimura, T. Kato, K. Ohya, T. Moriarty, K. Emery, C. Chen, J. Gao, G. Li, Y. Yang, *Nat. Commun.*, 2013, **4**, No. 1446; b) X. G. Guo, N. J. Zhou, S. J. Lou, J. Smith, D. B. Tice, J. W. Hennek, R. P. Ortiz, J. L. Navarrete, S. Y. Li, J. Strzalka, L. X. Chen, R. Chang, A. Facchetti, T. J. Marks, *Nat. Photon.*, 2013, **7**, 825; c) Y. F. Deng, W. L. Li, L. H. Liu, H. K. Tian, Z. Y. Xie, Y. H. Geng, F. S. Wang, *Energy Environ. Sci.*, 2015, **8**, 585.

4 a) T. Yang, M. Wang, C. Duan, X. Hu, L. Huang, J. Peng, F. Huang, X. Gong, *Energy Environ. Sci.*, 2012, **5**, 8208; b) K. Cnops, B. P. Rand, D. Cheyns, B. Verreet, M. Empl, P. Heremans, *Nat. Commun.*, 2014, **5**, No. 3406; c) Q. Zhang, B. Kan, F. Liu, G. K. Long, X. J. Wan, X. Q. Chen, Y Zuo, W. Ni, H. J. Zhang, M. M. Li, Z. C. Hu, F. Huang, Y. Cao, Z. Q. Liang, M. T. Zhang, T. Russell, Y. S. Chen, *Nat. Photon.*, 2015, **9**. 35.

5 a) D. Liu, M. Xiao, Z. Du, Y. Yan, L. Han, V. A. L. Roy, M. Sun, W. Zhu, C. S. Lee, R. Yang, *J. Mater. Chem. C*, 2014, **2**, 7523; b) Y. Chen, Y. Yan, Z. Du, X. Bao, Q. Liu, V. A. L. Roy, M. Sun, R. Yang, C. S. Lee, *J. Mater. Chem. C*, 2014, **2**, 3921; c) M. Löbert, A. Mishra, C. Uhrich, M. Pfeiffer, P. Bäuerle, *J. Mater. Chem. C*, 2014, **2**, 4879; d) M. Liu, Y. Liang, P. Chen, D. Chen, K. Liu, Y. Li, S. Liu, X. Gong, F. Huang, S. Su, Y. Cao, *J. Mater. Chem. A*,

2014, **2**, 321; e) Y. Chen, Z. Du, W. Chen, S. Wen, L. Sun,Q. Liu, M. Sun, R. Yang, *New J. Chem.*, 2014, **38**, 1559; f) A. Yassin, P. Leriche, M. Allain, J. Roncali, *New J. Chem.*, 2013, **37**, 502.

6 a) Y. J. He, H. Chen, J. H. Hou, Y. F. Li, *J. Am. Chem. Soc.*, 2010, **132**, 1377; b) Y. J. He, Y. F. Li, *Phys. Chem. Chem. Phys.*, 2011, **13**, 1970; c) C. Li, H. Yip, A. K. Y. Jen, *J. Mater. Chem.*, 2012, **22**, 4161; d) J. Wang, Z. He, H. Wu, Y. Cao, J. Pei, *New J. Chem.*, 2012, **36**, 1583.

7 a) R. Ross, C. Cardona, D. Guldi, S. G. Sankaranarayanan, M. Reese, N. Kopidakis, J. Peet, B. Walker, G. C. Bazan, E. Keuren, B. Holloway, M. Drees, *Nat. Mater.*, 2009, **8**, 208; b) C. Wang, W. Zhang, R. Horn, Y. Tu, X. Gong, S. Cheng, Y. Sun, M. Tong, J. Seo, B. Hsu, A. J. Heeger, *Adv. Mater.*, 2011, **23**, 2951; c) N. Tseng, Y. Yu, Y. Li, J. Zhao, S. So, H. Yan, K. M. Ng, *J. Mater. Chem. C*, 2015, **3**, 977.

8 a) P. Sonar, J. P. F. Lim, K. L. Chan, *Energy Environ. Sci.*, 2011, **4**, 1558; b) J. E. Anthony, *Chem. Mater.*, 2011, **23**, 583; c)A. Facchetti, *Mater. Today*, 2013, **16**, 123; d)Y. Lin, Y. Li, X. Zhan, *Adv. Energy Mater.*, 2013, **3**, 724; e) Y.Z. Lin, X. W. Zhan, *Mater. Horiz.*, 2014, **1**, 470; f) A. F. Eftaiha, J. Sun, I. G. Hill, G. C. Welch, *J. Mater. Chem. A*, 2014, **2**, 1201.

9 a) X. Zhang , Z. H. Lu , L. Ye , C. L. Zhan , J. H. Hou , S. Q. Zhang , B. Jiang, Y. Zhao , J. H. Huang , S. L. Zhang , Y. Liu , Q. Shi , Y. Q. Liu ,J. N. Yao, *Adv. Mater.*, 2013, **25**, 5791; b) P. Cheng, L. Ye, X. G. Zhao, J. H. Hou, Y. F. Li, X. W. Zhan, *Energy Environ. Sci.*, 2014, **7**, 1351; c) W. Jiang, L. Ye, X. G. Li, C. Y. Xiao, F. Tan, W. C. Zhao, J. H. Hou, Z. H. Wang, *Chem. Commun.*, 2014, **50**, 1024; d) L. Ye, W. Jiang, W. Zhao, S. Zhang, D. Qian, Z. H. Wang, J. H. Hou, *Small*, 2014, **10**, 4658.

10 a) Y. Z. Lin , J. Y. Wang , Z. G. Zhang , H. T. Bai , Y. F. Li , D. B. Zhu, X. W. Zhan, *Adv. Mater.*, 2015, **27**, 1170; b) Y. Z. Lin, Z. G. Zhang, H. T. Bai, J. Y. Wang, Y. H. Yao, Y. F. Li, D. B. Zhu, X. W. Zhan, *Energy Environ. Sci.*, 2015, **8**, 610.

11 a) Y. Zhou, Y. Dai, Y. Zheng, X. Wang, J. Wang, J. Pei, *Chem. Commun.*, 2013, **49**, 5802; b) H. Li, T. Earmme, G. Ren, A. Saeki, S. Yoshikawa, N. M. Murari, S. Subramaniyan, M. Crane, S. Seki, S. A. Jenekhe, *J. Am. Chem. Soc.*, 2014, **136**, 14589; c) H. Li , T. Earmme , S. Subramaniyan , S. A. Jenekhe, *Adv. Energy Mater.*, DOI: 10.1002/aenm.201402041.

12 a) S. Holliday, R. Ashraf, C. Nielsen, M. Kirkus, J. Röhr, C.g Tan, E. Collado-Fregoso, A. Knall, J. Durrant, J. Nelson, I. McCulloch, *J. Am. Chem. Soc.*, 2015, **137**, 898; b) W. Senevirathna, J. Liao, Z. Mao, J. Gu, M. Porter, C. Wang, R. Fernando, G. Sauvé, *J. Mater. Chem. A*, 2015, **3**, 4203..

13 a) Y. Liu , C. Mu , K. Jiang , J. Zhao , Y. Li , L. Zhang , Z. Li , J. Y. L. Lai , H. Hu , T. Ma , R. Hu , D. Yu , X. Huang , B. Z. Tang , H. Yan, *Adv. Mater.*, 2015, **27**, 1015; b) X. Zhang, C. L. Zhan, J. N. Yao, *Chem. Mater.*, 2015, **27**, 166; c) J. Zhao, Y. Li, H. Lin, Y. Liu, K. Jiang, C. Mu, T. Ma, J. Y. L. Lai, H. Hu, D. Yu, H. Yan, *Energy Environ. Sci.*, 2015, **8**, 520; d) Y. Zang, C. Z. Li, C. C. Chueh, S. T. Williams, W.Jiang, Z. H. Wang, J. S. Yu, A. Y. Jen, *Adv. Mater.*, 2014, **26**, 5708.

14 a) B. Walker, A. Tamayo, X. Dang, P. Zalar, J. H. Seo, A. Garcia, M. Tantiwiwat, T. Q. Nguyen, *Adv. Funct. Mater.*, 2009, **19**, 3063; b) S. Loser, C. J. Bruns, H. Miyauchi, R. P. Ortiz, A. Facchetti, S. I. Stupp, T. J. Marks, *J. Am. Chem. Soc.*, 2011, **133**, 8142; c) Y. Z. Lin, L. C. Ma, Y. F. Li, Y. Q. Liu, D. B. Zhu, X. W. Zhan, *Adv. Energy Mater.*, 2013, **3**, 1166.

15 a) L. Ye, S. Zhang, W. Ma, B. Fan, X. Guo, Y. Huang, H. Ade, J. H. Hou, *Adv. Mater.*, 2012, **24**, 6335; b) W. W. Li, K. H. Hendriks, W. S. C. Roelofs, Y. Kim, M. M. Wienk, R. A. J. Janssen, *Adv. Mater.*, 2013, **25**, 3182; c) W.W. Li, K. H. Hendriks, A. Furlan, W. S. C. Roelofs, M. M. Wienk, R. A. J. Janssen; *J. Am. Chem. Soc.*, 2013, **135**, 18942.

16 a) J. W. Rumer, S. Dai, M. Levick, Y. Kim, M. Madec, R. S. Ashraf, Z. Huang, S. Rossbauer, B. Schroeder, L. Biniek, S. E. Watkins, T. D. Anthopoulos, R. A. J. Janssen, J. R. Durrant, D. J. Procter, I. McCulloch, *J. Mater. Chem. C*, 2013, **1**, 2711; b) I. Meager, R. S. Ashraf, C. B. Nielsen, J. E. Donaghey, Z. Huang, H. Bronstein, J. R. Durrant, I. McCulloch, *J. Mater. Chem. C*, 2014, **2**, 8593; c) L. Zhang, S. Zeng, L. Yin, C. Ji, K. Li,Y. Li, Y. Wang, *New J. Chem.*, 2013, **37**, 632.

17 a) C. M. Yu, C. He, Y. Yang, Z. X. Cai, H. W. Luo, W. Q. Li, Q. Peng, G. X. Zhang, Z. T. Liu, D. Q. Zhang, *Chem. Asian J.*, 2014, **9**, 1570; b) C. M. Yu, Z. T. Liu, Y. Yang, J. J. Yao, Z. X. Cai, H. W. Luo, G. X. Zhang, D. Q. Zhang, *J. Mater. Chem. C*, 2014, **2**, 10101; c) Z. T. Liu, G. X. Zhang, Z. X. Cai, X. Chen, H. W. Luo, Y. H. Li, J. G. Wang, D. Q. Zhang, *Adv. Mater.*, 2014, **26**, 6965; d) J. J. Yao, Z. X. Cai, Z. T. Liu, C. M. Yu, H. W. Luo, Y. Yang, S. F. Yang, G. X. Zhang,D. Q. Zhang, *Macromolecules*, 2015, **48**, 2039.

18 Y. Yang, G. X. Zhang, C. M. Yu, C. He, J. G. Wang, X. Chen, J. J. Yao, Z. T. Liu, D. Q. Zhang, *Chem. Commun.*, 2014, **50**, 9939.

19 S. Loser, C. J. Bruns, H. Miyauchi, R. P. Ortiz, A. Facchetti, S. I. Stupp, T. J. Marks, *J. Am. Chem. Soc.*, 2011, **133**, 8142.

20 G. G. Malliaras, J. R. Salem, P. J. Brock, C. Scott, *Phys. Rev. B*, 1998, **58**, 13411.

21 a) T. Erb, U. Zhokhavets, G. Gobsch, S. Releva, B. Stuhn, P. Schilinsky, C. Waldauf, C. J. Brabec, *Adv. Funct. Mater.*, 2005, **15**, 1193; b) P. Vanlaeke, A. Swinnen, I. Haeldermans, G. Vanhoyland, T. Aernouts, D. Cheyns, C. Deibel, J. D'Haen, P. Heremans, J. Poortmans, J. V. Manc, *Sol. Energy Mater. Sol. Cells,* 2006, **90**, 2150.

22 M. Leung, M. B. Viswanath, P. Chou, S. Pu, H. Lin, B. Jin, *J. Org. Chem.*, 2005, **70**, 3560.